

Accounting for multiplicity in machine learning benchmark performance

Kajsa Møllersen

*Sami University of Applied Sciences,
Department of Computer Science
UiT — The Arctic University of Norway*

KAJSAM@SAMAS.NO

Einar Holsbø

*Department of Computer Science & CANS
UiT — The Arctic University of Norway*

EINAR.J.HOLSBO@UIT.NO

Editor:

Abstract

State-of-the-art (SOTA) performance refers to the highest performance achieved by some model on a test sample, preferably under controlled conditions such as public data (reproducibility) or public challenges (independent sample). Thousands of classifiers are applied, and the highest performance becomes the new reference point for a particular problem. In effect, this set-up is an estimate of the expected best performance among all classifiers applied to a random sample; a sample maximum estimate. In this paper, we argue that SOTA should instead be estimated by the expected performance of the best classifier, which can be done without knowing which classifier it is.

Our contribution is the formal distinction between the two, and an investigation into the practical consequences of using the former to estimate the latter. This is done by presenting sample maximum estimator distributions for non-identical and dependent classifiers. We illustrate the impact on real world examples from public challenges.

1 Estimating state-of-the-art performance

Machine learning (ML) models are commonly evaluated and compared by their performance on data sets from public repositories, where models can be evaluated under identical conditions and across time. Theoretical results play an important role in ML research, but for the last couple of decades the success of increasingly complex models has pushed the evidence towards performance on benchmark data sets. In this paper, we direct attention to the reporting of state-of-the-art (SOTA) performance. We restrict our attention to classifier performance, but the overall mechanisms apply to other models. The term performance will in general refer to quantification of the classifier's ability to correctly classify the instances in a sample, and we will specify when necessary. Other performance measures, such as computation time, will not be addressed here.

Because of the complexity of both models and their training and test samples, the performances are estimated by applying the models to data samples. Within the fields of research that develop, refine, test and use classifiers, the term SOTA commonly refers to the highest reported performance to date, and is used as a reference point when presenting and comparing models. The highest performance serves as an estimate of SOTA, although

the term “estimate” is seldom used explicitly. There is an important distinction between best performance among a number of classifiers, and performance of best classifier, and this paper makes an effort to bring attention to this distinction.

1.1 SOTA performance

SOTA refers to the best model, and hence SOTA performance is the performance of that model. Let $\Theta = \{\theta_1, \theta_2, \dots, \theta_m\}$ be the probability of success for m classifiers, and let $\hat{\theta}_j$, $j = 1, \dots, m$, be their corresponding unbiased estimates. In a public challenge, Θ would be the classifier performances of the m participants. Taking into account that the participants of a challenge is somewhat arbitrary, and that their classifiers are adjusted to a training sample, we model the classifier ensemble as random sample where $\theta_j \sim P(\theta)$, and define SOTA performance as follows

Definition 1 (SOTA classifier performance) Let θ_j be the random variable that denotes the performance of classifier j . In an ensemble of m classifiers with performances $\Theta = \{\theta_1, \theta_2, \dots, \theta_m\}$, the SOTA classifier performance is the expected best performance

$$\theta_{SOTA} = E \max \Theta. \quad (1)$$

For non-random classifier ensembles, the definition holds since the expectation of a constant is just the constant itself, $\theta_{SOTA} = \max \Theta$. This definition answers the question *what can we expect the best classifier’s performance to be?*, when applied to a new data sample. Note that picking the highest estimated performance derived from an ensemble of classifiers applied to a test sample does not answer this question.

1.2 Sample maximum performance

ML models are commonly ranked by their performance on benchmark datasets, published as leaderboards, often in public challenges where the test sample is withheld to avoid overfitting. The best performance to date, or among the participants in a challenge, is referred to as SOTA, see, for example paperswithcode.com. The published performances are estimates, $\hat{\theta}_j$ ’s, based on the application of models on a specific benchmark or test sample. Although seldom formalised, these are often unbiased estimates, and we will treat them as such. The test samples act as random samples, all the while the point of reporting these performances is the assumption that they can be generalised to similar data sets. Hence, the $\hat{\theta}_j$ ’s are a random sample, and the best performance is the sample maximum estimate, which we define for clarity.

Definition 2 (Sample maximum estimator) Let θ_j be the random variable that denotes the performance of classifier j and let $\hat{\theta}_j(X)$ be the corresponding unbiased estimator. For an ensemble of m classifiers with performances $\Theta = \{\theta_1, \theta_2, \dots, \theta_m\}$, the sample maximum performance estimator is

$$\hat{\theta}_{\max}(\mathbf{X}) = E \max(\hat{\Theta}(\mathbf{X})), \quad (2)$$

where $\mathbf{X} = \{X_1, X_2, \dots, X_m\}$ quantifies successes for classifiers $j = 1, \dots, m$.

The sample maximum answers the question *What is the best expected performance of an ensemble of classifiers?* When $\hat{\theta}_{\max}(\mathbf{X})$ is used as an estimator for θ_{SOTA} , it is biased. The two terms look similar at a glance, the only thing distinguishing them are $\hat{\Theta}(\mathbf{X})$ vs Θ . Taking into account that $\hat{\theta}(X)$ is an unbiased estimator for θ , the distinction can easily be overlooked. The difference reflects a multiplicity effect.

1.3 Multiplicity effect

Multiplicity is, simply put, how the probability of an outcome changes when an experiment is performed multiple times. As we will show in the subsequent sections, using the maximum performance of an ensemble as an estimate for SOTA is a biased estimator giving overoptimistic results. The bias is a multiplicity effect; multiple models being applied to the same sample.

The optimistic estimate is often used as a reference point for evaluating new models. Not to say that a new model necessarily needs to beat the current SOTA to catch interest from reviewers and editors, but it certainly helps if its performance is comparable. Many aspects of public benchmark datasets and public challenges have been thoroughly discussed, and we present some of the topics connected to multiplicity in Section 2. As far as the authors are aware of, the multiplicity effect has been nearly absent from the discussion regarding SOTA estimates.

We present the sample maximum estimator distribution function and its bias for some classifier scenarios. In its simplest form, independent classifiers with identical probability of success, the distribution function of the sample maximum estimator exists in closed form. With growing complexity, such as mutual dependencies and more elaborate performance measures, the distribution function of the estimator is no longer known, but the mechanisms at play and the pitfalls to be aware of are much the same, and limited studies can be done by straightforward simulations. We demonstrate the impact of multiplicity through simulated examples, and show how classifier dependency impacts bias and variance.

Finally, we discuss three real-world examples that each highlights different aspects of multiplicity and SOTA estimation. From these real-world examples, we suggest a SOTA estimate, in line with Definition 1. This is a new perspective for multiplicity effects in the ML context, a step aside from overfitting and re-use of test sets.

All code is available at <https://github.com/3inar/ninety-nine>.

2 Related work

Multiple comparisons is a well-studied subject within statistics, see, for example, Tukey (1991) for an interesting discussion on some topics, among them confidence intervals (CIs). For a direct demonstration of how multiple testing can lead to false discoveries, Bennett et al. (2009) gave an example where brain activity is detected in (dead) salmon “looking” at photos of people. In the ML context, with multiple data sets and classifiers, Demšar (2006) suggested adjusting for multiple testing, according to well-known statistical theory. This paper focuses on the estimate itself and its uncertainty, and not comparison of methods.

The use and re-use of benchmark datasets has been addressed in several publications. Longjohn et al. (2025) drew attention to the role of data repositories with leaderboards and their lack of metric uncertainty. Salzberg (1997) pointed to the problem that arises because

these datasets are static, and therefore run the risk of being exhausted by overfitting. Exhausted public data sets still serve important functions, for example, a new idea can show to perform satisfactory, even when it is not superior. Thompson et al. (2020) distinguished between simultaneous and sequential multiple correction procedures. In sequential testing, which is the reality of public datasets, the number of tests is constantly updated. An interesting topic they bring up is the conflict between sharing incentive, open access and stable false positive rate. There are several demonstrations of the vulnerability of re-use of benchmark datasets. Teney et al. (2020) performed a successful attack on the VQA-CP benchmark dataset (introduced by Agrawal et al., 2018); they were able to attain high performance with a non-generalisable classifier. They point towards the risk of ML methods capturing idiosyncrasies of a dataset. Torralba and Efros (2011) introduced the game Name That Dataset! motivating their concern of methods being tailored to a dataset rather than a problem. The lack of statistically significant differences among top performing methods is demonstrated by, for example, Everingham et al. (2015) and Fernández-Delgado et al. (2014).

The same mechanisms of overfitting are present in public challenges through multiple submissions on the validation sample. Blum and Hardt (2015) introduced an algorithm that releases the public leaderboard score only if there has been significant improvement compared to the previous submission. This will prevent overfitting by hindering adjustments to random fluctuations in the score and not true improvements of the method. Dwork et al. (2017) used the principles of differential privacy to prevent overfitting to the validation set.

Several publications show that the overfitting is not as bad as expected, and provide possible explanations. Recht et al. (2019) constructed new, independent test sets of CIFAR-10 and ImageNet. They found a dramatic drop in accuracy, around 10%. However, the order of the best performing methods is preserved, which can be explained by the fact that multiple classes (Feldman et al., 2019) and model similarity (Mania et al., 2019) slow down overfitting. Roelofs et al. (2019) compared the results from the private leaderboard (one submission per team) and the public leaderboard (several submissions per team) in Kaggle challenges. Several of their analyses indicate overfitting even though their main conclusion was that there is little evidence of overfitting.

Overfitting and its consequences are avoided in most challenges by withholding the test sample so that a method can only be evaluated once and not adapted to the result. Hold-out datasets also prevents wrong use of cross-validation, see, for example, Fernández-Delgado et al. (2014) and the seminal paper of Dietterich (1998). Another contribution from public challenges is the requirement of reproducibility to collect the prize money, which is a well-known concern in science, see, for example, Gundersen and Kjensmo (2018). Public challenges typically rank the participants by a (single) performance measure, and can fall victims of Goodhart’s law, paraphrased as “When a measure becomes a target, it ceases to be a good measure.” by Teney et al. (2020). Møllersen et al. (2017) demonstrated how five different performance measures completely rearranges the leaderboard for the top participants in the ISBI 2016 challenge Skin Lesion Analysis towards Melanoma Detection (Gutman et al., 2016). Ma et al. (2021) offered a framework and platform for evaluation of NLP methods, where other aspects such as memory use and robustness are evaluated.

The robustness of a method, and the variability in performance are crucial aspects that the hold-out test set of public challenges do not offer an immediate solution to. Bouthillier

et al. (2021) showed empirically that hyperparameter choice and the random nature of the data are two large contributors to variance, whereas data augmentation, dropouts, and weights initialisations are minor contributors. Choice of hyperparameters are often adjusted to validation set results, and the strategies of Blum and Hardt (2015) and Dwork et al. (2017) can hinder that, if implemented by the challenge hosts.

Our contribution is a focus on better estimate for SOTA performance under the current conditions, where the approach of Bouthillier et al. (2021) does not apply. Bousquet and Elisseeff (2002) investigated how sampling randomness influences accuracy, both for regression algorithms and classification algorithms, relying on the work of Talagrand (1996) who stated that “A random variable that depends (in a “smooth” way) on the influence of many independent variables (but not too much of any of them) is essentially constant.”

There is a rich literature on various aspects regarding the use of public challenges as standards for scientific publications, see, for example, Varoquaux and Cheplygina (2022) for a much broader overview than the one given here. We contribute to this conversation by shining the light on how multiplicity of classifiers’ performance on hold-out test sets create optimistic estimates of SOTA performance.

3 Multiple classifiers and biased state-of-the-art estimation

In the following sections, we take a closer look at the sample maximum estimator by presenting its distribution and investigating its bias and variance when used for SOTA estimation. We wrap the presentation in a public challenge context to refer back to previous work presented in Section 2. We use standard deviation instead of variance, because standard deviation is below 0.005 for our numerical examples. We use the following default parameter values: $n = 3,000$, $\theta = 0.90$, and $m = 1,000$, $\theta_{SOTA} = 0.9$.

3.1 Notation and parameter values

n	: number of trials/size of test sample
θ	: probability of success
m	: number of experiments/size of classifier ensemble
$\mathcal{Bern}(\theta)$: Bernoulli distribution
Y	: indicator variable for success
$Y \sim \mathcal{Bern}(\theta)$	
$\mathcal{B}(n, \theta)$: binomial distribution
X	: number of successes
$X \sim \mathcal{B}(n, \theta)$	
$\hat{\theta}(X) = \frac{X}{n}$: estimator for θ
$P(X = x)$: probability of x successes
$P_x = P(X \leq x)$: probability of at most x successes
$\mathbf{X} = \{X_1, X_2, \dots, X_m\}$: number of successes for classifiers $j = 1, \dots, m$
C_x	: number of classifiers with at most x successes
$C_x \sim \mathcal{B}(m, P_x)$	
$\Theta = \{\theta_1, \theta_2, \dots, \theta_m\}$: probability of success for classifiers $j = 1, \dots, m$
$\theta \sim P(\theta)$	
$\Theta' = \{\theta'_1, \theta'_2, \dots, \theta'_m\}$: empirical Bayes estimate for $P(\theta)$
$\hat{\Theta}(\mathbf{X}) = \{\hat{\theta}_1(X_1), \hat{\theta}_2(X_2), \dots, \hat{\theta}_m(X_m)\}$: estimator for Θ
$\theta_{SOTA} = E \max(\Theta)$: expected highest probability of success
$\hat{\theta}_{\max}(\mathbf{X}) = \max(\hat{\Theta}(\mathbf{X}))$: sample maximum estimator

We use simplified notation, for example, $E\hat{\theta}(X)$ is written $E\hat{\theta}$, when there is no risk of confusion.

Some of the expectations, standard deviations and distributions need to be estimated by simulations. In the hierarchical set-up, we use $B = 1,000$ draws from $P(\theta)$ in Eq. 1b, and $rep = 100,000$ when drawing random samples of \mathbf{X} for each θ_j . We denote the estimates without the “hat”, leaning on the Law of Large Numbers and the access to arbitrary large B and rep .

We refer to classifiers with identical probability of success as identical classifiers. We use significance level $\alpha = 0.05$ and two-sided CIs.

3.2 The invention of a coin-flip classifier

We here give a motivating example, related to multiple testing, to illustrate the effect of multiplicity. For any classifier that predicts the outcome of the flip of a fair coin, the probability of success is 0.5, and hence the SOTA performance is $\theta_{SOTA} = 0.5$. If we had

a public challenge where the aim was to make a coin-flip classifier, what would the SOTA performance be?

Consider an experiment where a classifier predicts the outcome of a fair coin being flipped $n = 20$ times. Let the random variable X denote the number of successes, $X \sim \mathcal{B}(n, \theta)$, and let $\hat{\theta}(X) = X/n$. We are interested in the probability of observing a large $\hat{\theta}$, say, ≥ 0.90 , and wrongfully getting the impression that a coin-flip classifier has been invented. For a single classifier, this is calculated from $1 - P(X \leq x|n, \theta)$, which in our example gives us a probability of 0.00020, reasonably low for making the false claim of coin-flip classifier invention.

For the multiplicity setting with m independent classifiers, define the “success” of a classifier as $\{X \leq x\}$. Each classifier is then a Bernoulli trial. Let C_x be the random variable that denotes the number of classifiers with success. We have that $C_x \sim \mathcal{B}(m, P_x)$, where $P_x = P(X \leq x|n, \theta)$. Of special interest in this example is one or more classifiers performing at 0.90 or above, defined as “failure” in this set-up. This can be written as $1 - P(C_x = m) = 1 - P_x^m$. P_x^m is equivalent to the probability of the sample maximum, or the m th order statistic, for random samples. With $m = 1,0000$ classifiers, the probability of at least one classifier performing at 0.90 or above is 0.18, a substantial risk of grossly overestimating θ_{SOTA} .

The same mechanism as described here is present when highest model performance is reported from public challenge leaderboards or public data sets. Even without the usual suspects of data re-use, overfitting, wrong use of cross-validation, multiple testing or data leakage, multiplicity, when not properly accounted for, can give the impression of the invention of a coin-flip classifier.

3.3 The probability distribution of $\hat{\theta}_{\max}(\mathbf{X})$

Let $\Theta = \{\theta_1, \theta_2, \dots, \theta_m\}$ be the probability of success for m classifiers, and let $\mathbf{X} = \{X_1, X_2, \dots, X_m\}$ be the set of random variables that denotes the number of successes (correct predictions) for each classifier on a sample of size n . Let the statistic $\hat{\theta}_{\max}(\mathbf{X}) = \max(\{\hat{\theta}_1(X_1), \hat{\theta}_2(X_2), \dots, \hat{\theta}_m(X_m)\})$ be the naive sample maximum estimator for θ_{SOTA} . We are interested in the probability distribution of $\hat{\theta}_{\max}(\mathbf{X})$.

In the coin-flip example, the θ_j ’s were equal and fixed, but we can generalize to $\theta_j \sim P(\theta)$, where the m classifiers from where \mathbf{X} originates are themselves a random sample. We can model the probability mass function (pmf) as a hierarchical distribution as follows:

$$\hat{\theta}_{\max}(\mathbf{X}) | \Theta \sim P(\hat{\theta}_{\max}(\mathbf{X}) | \Theta) \quad (1a)$$

$$\theta_j \sim P(\theta). \quad (1b)$$

The sampling procedure is illustrated in Figure 1.

The sample maximum is equivalent to at least one classifier having more than x correct predictions, and can be written as $1 - P(\hat{\theta}_{\max}(\mathbf{X}) \leq x/n)$, which in turn corresponds to $1 - F(x|\Theta)$. In the case where Θ is fixed the hierarchical distribution reduces to Eq. 1a, and we denote it simply by $F(x)$. We will continue this section with fixed Θ , and introduce random Θ in Section 4.

We first present identical and independent classifiers, for which the sample maximum estimator is just a special case of the order statistic. We have the following cumulative

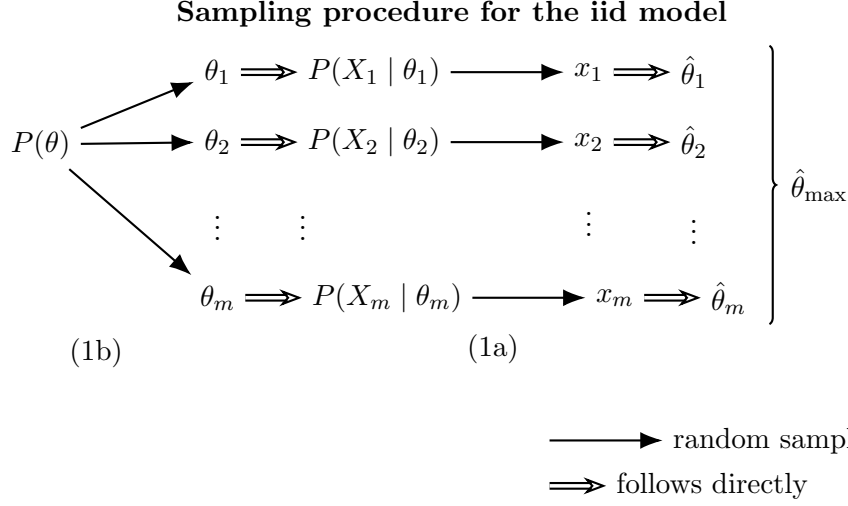


Figure 1: The θ_j 's are sampled from $P(\theta)$. The x_j 's are then sampled from their respective distributions, and $\hat{\theta}_{\max}$ follows directly.

distribution function (cdf):

$$F(x) = P_x^m = P(X \leq x)^m = \left(\sum_{\ell=0}^x P(X = \ell) \right)^m, \quad (2)$$

and the corresponding pmf:

$$\begin{aligned}
 f(x) &= P_x^m - P_{x-1}^m \\
 &= \left(\sum_{\ell=0}^x P(X = \ell) \right)^m - \left(\sum_{\ell=0}^{x-1} P(X = \ell) \right)^m \\
 &= \sum_{k=0}^{m-1} \binom{m}{k} \left(\sum_{\ell=0}^{x-1} P(X = \ell) \right)^k P(X = x)^{m-k}
 \end{aligned} \quad (3)$$

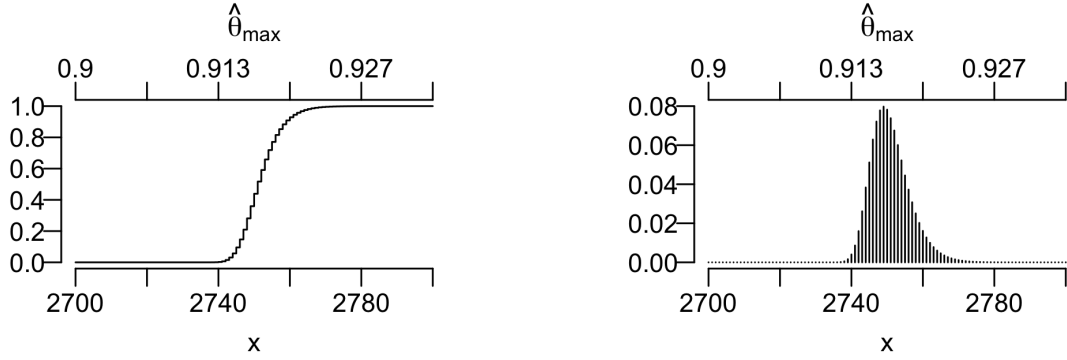
where $f(x = 0) = F(x = 0)$. See Casella and Berger (2002, p. 228) for details. Figure 2 shows an example with default parameter values.

3.4 A simulated public challenge

Consider a public challenge consisting of a classification problem on a test sample of size $n = 3,000$, and $m = 1,000$ participants. Let the classifiers be independent with identical probability of success, $\theta = 0.90$, and hence $\theta_{SOTA} = 0.90$. The classifier with the highest performance, $\hat{\theta}$, is declared winner, commonly referred to as SOTA. Figure 3 illustrates the slim chances a single better classifier has of beating an ensemble of worse classifiers.

In Figure 3, the blue curve shows the pmf of a single $\hat{\theta}(X)$. The CI of $\hat{\theta} = E\hat{\theta} = \theta$, denoted by $(\theta_{\alpha/2}, \theta_{1-\alpha/2})$, is the blue line on the horizontal axis. If we take multiplicity into account, the expected performance, in terms of sample maximum for the $m = 1,000$

Cdf and pdf for identical, independent classifiers


 (a) Cdf $F(x)$, see Eq. 2

 (b) Pmf $f(x)$, see Eq. 3

Figure 2: The cdf and pmf of the sample maximum estimator for $n = 3,000$, $\theta = 0.90$, and $m = 1,000$. The horizontal axes denotes the number of successes, x , at the bottom and the corresponding sample maximum estimates, $\hat{\theta}_{\max}$, at the top.

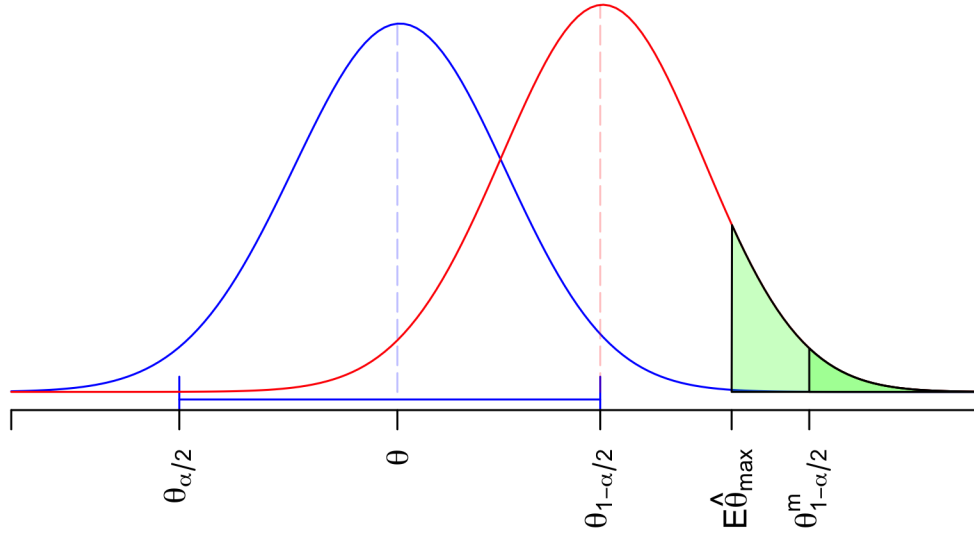
 The pmfs of two single $\hat{\theta}(X)$ compared to the $\hat{\theta}_{\max}$ statistics


Figure 3: The blue and the red curves show the pmfs of $\hat{\theta}(X)$ for classifiers with probability of success θ and $\theta_{1-\alpha/2}$, respectively. $\theta_{1-\alpha/2}$ is the upper limit of the CI of $\hat{\theta}(x) = \theta$. The CI is the blue horizontal line. $E\hat{\theta}_{\max}$ and $\theta_{1-\alpha/2}^m$ denote the expected value of $\hat{\theta}_{\max}$ and the upper limit of the corresponding CI for $m = 1,000$ classifiers. The green shaded areas are $P(\hat{\theta}_{m+1} \geq \theta_{1-\alpha/2}^m)$ and $P(\hat{\theta}_{m+1} \geq E\hat{\theta}_{\max})$.

participating teams, is $E \hat{\theta}_{\max} = 0.9173$, indicated on the horizontal axis together with the upper limit of its CI, denoted as $\theta_{1-\alpha/2}^m$.

Consider a new classifier with probability of success $\theta_{m+1} = \theta_{1-\alpha/2}$. The corresponding pmf is displayed as the red curve in Figure 3, with the dotted line indicating $E \hat{\theta}_{m+1} = \theta_{1-\alpha/2}$. By common scientific standards, a classifier performance of $\hat{\theta} = \theta_{m+1}$ is considered significantly better than a performance of $\hat{\theta} = \theta$, but the multiplicity effect can conceal this.

The probability of the new and better classifier beating the ensemble of worse classifiers is low: $P(\hat{\theta}_{m+1} \geq E \hat{\theta}_{\max}) = 0.10$, displayed as the green areas under the red curve. This means that by using the sample maximum as an estimator for SOTA, we can expect that 9 out of 10 classifiers that are significantly better will still be naively considered worse.

The distribution of $\hat{\theta}_{\max}(\mathbf{X})$ for these default parameters is displayed in Figure 2. To get an insight in how the parameter values impacts the distribution, Figure 4 shows the bias and standard deviation of $\hat{\theta}_{\max}(\mathbf{X})$ as a function of m , n and θ , respectively.

In Figure 4a, we see that the impact of number of classifiers is dramatic, and multiplicity considerations must be treated with full attention starting at $m = 2$. Figure 4c demonstrates that the test set size also has large impact on the bias, which can be traced back to the standard error, $\sqrt{\theta(1-\theta)/n}$. The standard error also explains the decrease in bias as θ approaches 1, as seen in Figure 4e: The standard deviation of the individual $\hat{\theta}_j(X)$'s is at its highest for $\theta = 0.5$ and decreases monotonically.

Figures 4b, 4d and 4f show the corresponding standard deviations. For numerical values, see Table 3 in Appendix A.

4 Non-identical θ 's and classifier dependency

The probability distribution in Section 3.4 is that of independent classifiers with identical θ 's, an assumption that is rarely true in practice. We expand our investigation to non-identical θ 's and classifier dependency, non-iid for short. We model this as the hierarchical distribution presented in Section 3.3:

$$\hat{\theta}_{\max}(\mathbf{X}) | \Theta \sim P(\hat{\theta}_{\max}(\mathbf{X}) | \Theta, m, n, \rho) \quad (1a)$$

$$\theta_j \sim P(\theta), \quad (1b)$$

where m, n, ρ are fixed, and ρ is the correlation coefficient, see Section 4.2. In this model, the classifiers are a random sample from the distribution $P(\theta)$. θ_{SOTA} is no longer a fixed number, but defined as the expected maximum, $\theta_{SOTA} = E \max(\Theta)$.

For the demonstrations in the following subsections we will use $\theta \sim \mathcal{U}(a, b)$, the continuous uniform distribution, for which the sample maximum statistic, T , has probability density function (pdf)

$$f(t) = \frac{m(t-a)^{m-1}}{(b-a)^m},$$

and expected value

$$\theta_{SOTA} = E \max(\Theta) = ET = \frac{mb+a}{m+1}.$$

The bias and standard deviation of the sample maximum estimator

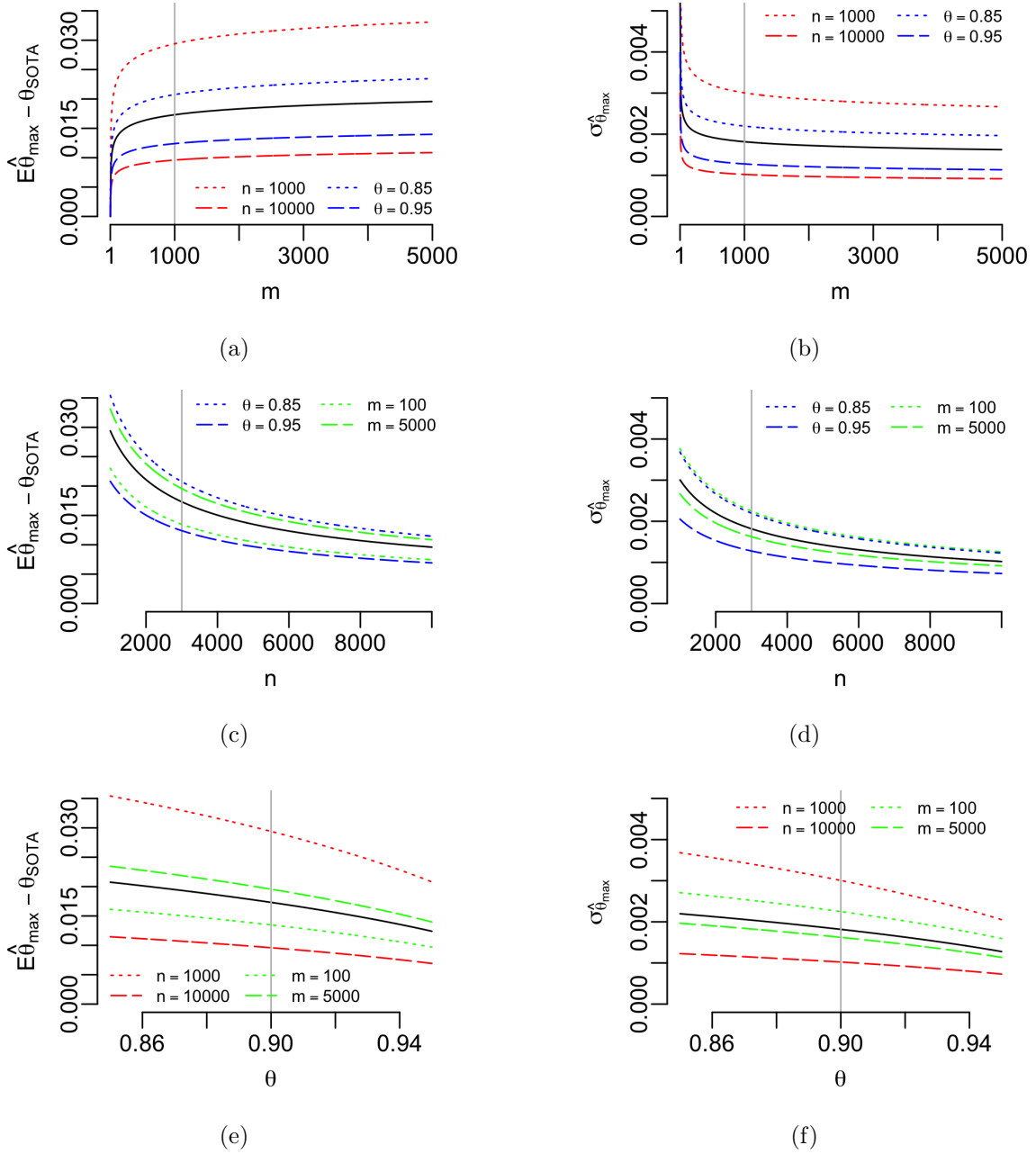


Figure 4: Bias and standard deviation of $\hat{\theta}_{\max}(\mathbf{X})$ as a function of each of its three parameters. For the black lines, two parameters are set to the default values $n = 3,000$, $\theta = 0.9$ and $m = 1,000$; the third is on the x-axis. The other lines represent offsets, with values displayed in the legends. Intersections with the gray vertical lines correspond to entries in Table 3 in Appendix A.

We use the set-up from Section 3.4 with $m = 1,000$ classifiers, test set size $n = 3,000$ and $\theta_{SOTA} = 0.90$. We have that $E \max \hat{\Theta}(\mathbf{X}) = E(E(\max \hat{\Theta}(\mathbf{X})|\Theta))$, and use Monte Carlo integration for the calculations.

Table 1 and Figure 5 give an overview of some exemplifying models, details are in the following sections.

Overview of $\hat{\theta}_{\max}(\mathbf{X})$ for dependent and non-identical classifiers

Section	Independent	Identical	Upper 95% CI	$E \hat{\theta}_{\max}$	$\sigma_{\hat{\theta}_{\max}}$
3.4	YES	YES	0.9213	0.9173	0.0018
4.1	YES	NO	0.9177	0.9129	0.0021
4.2	NO	YES	0.9207	0.9140	0.0035
4.3	NO	NO	0.9173	0.9101	0.0036

Table 1: The upper bound of the CI, the expected value and standard deviation for $\hat{\theta}_{\max}(\mathbf{X})$ for different combinations of independency and identicality. $\theta_{SOTA} = 0.90$, $n = 3,000$, $m = 1,000$. The correlation coefficient and $P(\theta)$ are found in their respective subsections.

Overall, Table 1 demonstrates that dependency and non-identical θ s reduce the bias of the $\hat{\theta}_{\max}(\mathbf{X})$ estimator, and assumptions regarding dependency and identicality are crucial to include in a model. Figure 5 shows how the bias and standard deviation change as functions of Θ and ρ_0 for these models.

4.1 Non-identical, independent classifiers

We are interested in generalising Eq. 2 to the non-identical case. We start by noting that we now have $P_{xj} = P(X \leq x|\theta_j)$, and we seek the sum of those so that we can find the proper expression for $F(x|\Theta) = P(C_x = m|\Theta)$.

The Poisson Binomial distribution describes the sum of m non-identical independent Bernoulli trials with success probabilities p_1, p_2, \dots, p_m (Wang, 1993). The pmf for K number of successes is

$$P(K = k) = \sum_{A \in G_k} \prod_{j \in A} p_j \prod_{i \in A^c} (1 - p_i),$$

where G_k is all subsets of size k that can be selected from $\{1, 2, \dots, m\}$. G_m contains only one subset $A = \{1, 2, \dots, m\}$, and its complement A^c is empty.

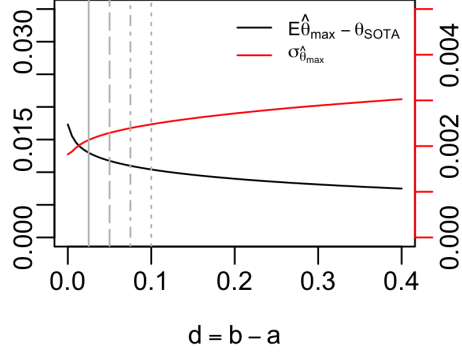
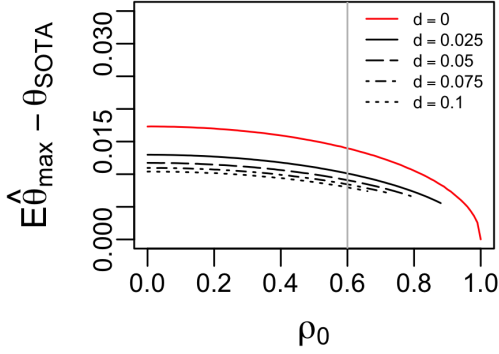
We get the following cdf for non-identical classifiers:

$$F(x|\Theta) = \sum_{A \in G_m} \prod_{j \in A} P_{xj} \prod_{i \in A^c} (1 - P_{xi}) = \prod_{j=1}^m P_{xj}. \quad (4)$$

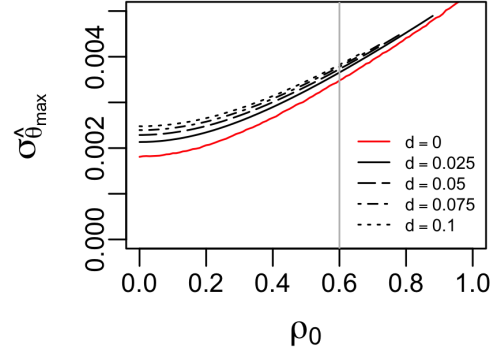
The corresponding pmf is

$$\begin{aligned} f(x|\Theta) &= \prod_{j=1}^m P_{xj} - \prod_{j=1}^m P_{x-1j} \\ &= \prod_{j=1}^m \sum_{k=0}^x \binom{n}{k} \theta_j^k (1 - \theta_j)^{n-k} - \prod_{j=1}^m \sum_{k=0}^{x-1} \binom{n}{k} \theta_j^k (1 - \theta_j)^{n-k}. \end{aligned} \quad (5)$$

Bias and standard deviation for non-iid classifiers


 (a) Bias and standard deviation as a function of $b - a$ in $\mathcal{U}(a, b)$


(b) Bias as a function of correlation coefficient.



(c) Standard deviation as a function of correlation coefficient.

Figure 5: Bias and standard deviation for $\hat{\theta}_{\max}(\mathbf{X})$ as a function of $d = b - a$ in $\mathcal{U}(a, b)$ for non-identical classifiers and of ρ_0 for conditional independent classifiers. The scale of the y -axes are kept the same as in Fig. 4 for easier comparison. (a) The left tip of the curve is identical classifiers. The support of $\mathcal{U}(a, b)$ stretches out along the x -axis, and the bias decreases. The intersection with the solid vertical line corresponds to the cdf and pmf in Fig. 6, and row 2 in Table 1. The intersections with the broken lines correspond to the left tips of the black lines in Fig. 5b where the classifiers are independent. (b) The red line is identical classifiers, discussed in Section 4.2. The left tip of the red curve corresponds to the iid classifiers in Section 3.4, and the intersection with the vertical line corresponds to row 3 in Table 1. The black lines show bias as a function of correlation coefficient demonstrated for different d 's. The intersection between the solid black curve and the grey vertical line corresponds to row 4 in Table 1. (c) The corresponding standard deviation.

Analytically, it is more complex than the case of identical classifiers, but it is easy to simulate. An example of cdf and pmf are displayed in Figure 6.

From row 2 in Table 1 we see that the bias is smaller, but the standard deviation is larger compared to the iid case. In our case, we can see this as the classifiers at the lower end not

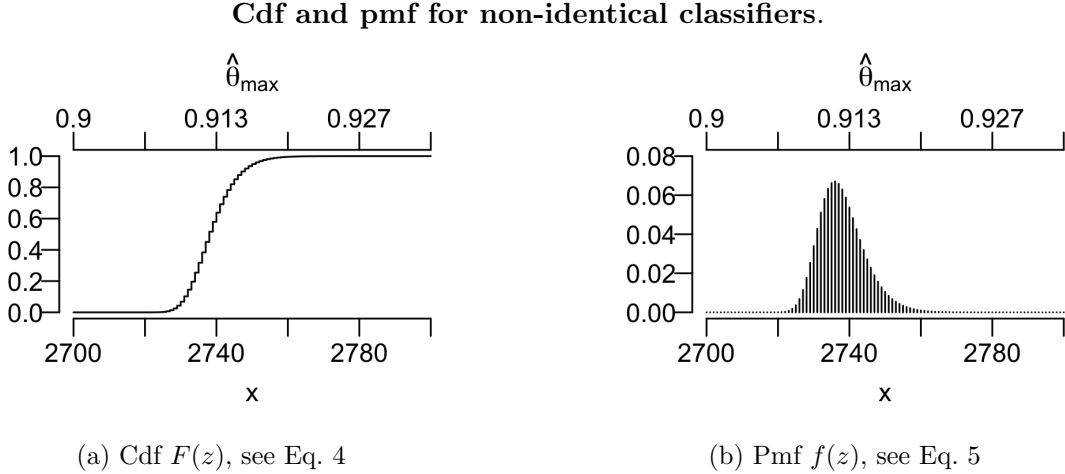


Figure 6: The distribution and the probability function of $\hat{\theta}_{\max}(\mathbf{X})$ for non-identical θ 's, with $\theta_j \sim \mathcal{U}(a, b)$ where $d = b - a = 0.025$. See Fig. 2 for the corresponding distributions for identical classifiers.

contributing to the sample maximum, and the reduced number of contributing classifiers gives a higher variance. The exact reduction/increase in bias and variance depends on $P(\theta)$, and can at its most extreme completely eradicate the multiplicity effect, as we shall see in Section 5.1.2.

Figure 5a shows how bias and standard deviation changes with d for fixed $\theta_{SOTA} = 0.90$. The bias decreases rapidly at first, but the rate goes down fast. This means that taking into account that classifier performances are heterogeneous is important, and even small variations from identity can have great impact on SOTA estimation. In Section 5, we demonstrate for other Θ s, based on observations.

4.2 Identical, dependent classifiers

Even though the different teams work independently, their resulting classifiers are not necessarily statistically independent. A classifier's ability to perform better than random guesses is due to dependencies between features and labels in the training sample. In their training phase, different classifiers will pick up on many of the same features and dependencies, regardless of which classifier they train. In addition, many teams will use different versions of related models, often pre-trained on the same data set. This scenario can be modelled by conditional independency.

Let Y_0 be a Bernoulli variable with $P(Y_0 = 1) = \theta_0$. Let Y_j be the Bernoulli variable with value 1 if classifier j predicts a data point correctly with $P(Y_j = 1) = \theta_j$, and let $j = 1, \dots, m$ be the m classifiers contributing to $\hat{\theta}_{\max}$. Boland et al. (1989) described dependency in the majority systems context, where $\rho_{0j} = \text{corr}(Y_0, Y_j)$, $j = 1, \dots, m$, and the Y_j s are independent given Y_0 . Y_0 does not contribute directly to $\hat{\theta}_{\max}$, but can be seen as, for example, the influence that a common training sample has on the classifiers.

The binomial distribution for dependent Bernoulli trials is not an easy problem, see, for example, Ladd (1975) and Hisakado et al. (2006). We can model the pmf as a hierarchical

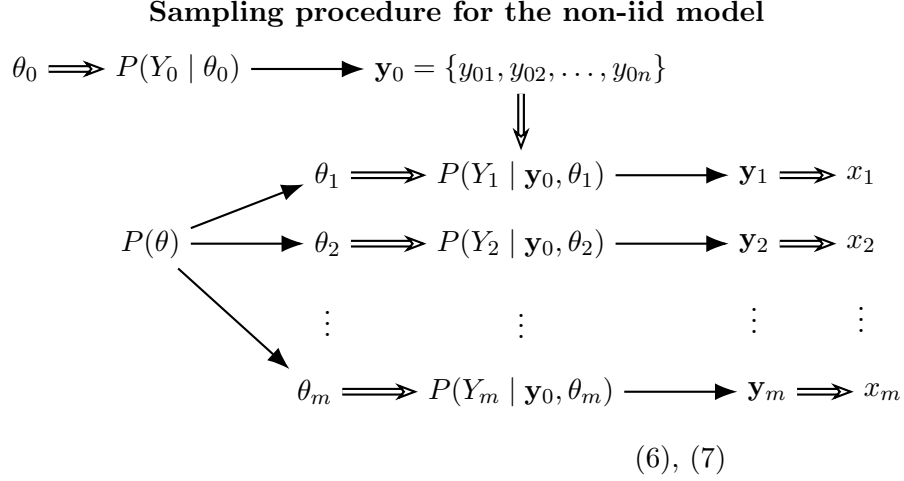


Figure 7: The parameter θ_0 defines the distribution from which the Y_0 's are sampled. The θ_j 's are sampled from $P(\theta)$ as in Fig. 1. Random samples of Y_j s are taken from their respective distributions, and x_j follows directly, which in turn gives $\hat{\theta}_{\max}(\mathbf{X})$ as in Fig. 1. $P(Y_j | \mathbf{y}_0, \theta_j)$ is described in Eq. 6 and 7.

distribution:

$$\begin{aligned} \hat{\theta}_{\max}(\mathbf{X}) | \Theta, Y_0 &\sim P(\hat{\theta}_{\max}(\mathbf{X}) | \Theta, Y_0) \\ \theta &\sim P(\theta), Y_0 \sim P(Y_0 | \theta_0). \end{aligned}$$

The Bernoulli trials can be simulated, see Boland et al. (1989) for conditional distributions. The sampling procedure is shown in Figure 7, illustrating the dependency step between the θ_j 's and the x_j 's in Figure 1.

We give an example for the case where $\rho_{0j} = \rho_0$ and $\theta_j = \theta$ for all classifiers, setting ρ_0 based on the work of Mania et al. (2019).

Mania et al. (2019) calculated model similarity, defined as the probability of two classifiers giving the same output, which is equivalent to

$$(1 - \theta_j)(1 - \theta_k) + \theta_j\theta_k + 2\rho_{jk}\sqrt{\theta_j\theta_k(1 - \theta_j)(1 - \theta_k)}$$

for models with correlation ρ_{jk} . The average accuracy for top-performing ImageNet models, $\hat{\theta} = 0.756$, and the calculated similarity of 0.85 gives $\rho = 0.36$ under the assumption of equal correlation for all classifiers. We have that $\rho_{jk} = \rho_{0j}^2$, and hence our proposed correlation ρ_0 is set to 0.6. Note that, for $\theta = 0.90$, the similarity as described by Mania et al. (2019) is 0.82 for two independent classifiers. When the probability of correct prediction is high, there is little room for variation between classifier outcomes.

Let $\theta = 0.90$ for all classifiers, and $\theta_0 = 0.90$. Comparing rows 1 and 3 in Table 1, we see a decrease in bias compared to the iid classifiers. However, the standard deviation has increased due to the random nature of Y_0 , so the upper CI is essentially the same.

To give an idea of how the randomness of Y_0 influences the standard deviation, we fix the y_0 's with exactly $\theta_0 = 0.90$ correct predictions. The expected value is the same as with

random Y_0 s, but the standard deviation has now decreased from 0.0035 to 0.0015. For real datasets, the dependencies have both random and fixed sources. The training and the test samples are random sources, a fixed source could be pre-trained models.

For $\rho_{0j} = 0$, we have independent classifiers, the same scenario as in Section 3.4, and for $\rho_{0j} = 1$, we have m classifiers producing the same output, and multiplicity is not a concern. For the whole range, see the red curve in Figure 5b. We see here that the correlation coefficient value in a model has a great impact on the estimated bias if the correlation is substantial. This can explain that in mature fields, where most competing teams will use variants of the same model, the multiplicity will not impact the overestimation of SOTA as much as in young fields where the competing teams have more diverse models. This aligns with what is often observed: overoptimistic results in the beginning, and more sober as the field evolves.

4.3 Non-identical, dependent classifiers

The most complex, but also the most realistic case, is when classifiers are non-identical and dependent. An analytical solution is not known (Hisakado et al., 2006), but simulations are straightforward. The results of Boland et al. (1989) can be extended, and we have that

$$P(Y_j|Y_0 = 1) = \frac{\rho\sqrt{\theta_j(1-\theta_j)\theta_0(1-\theta_0)} + \theta_j\theta_0}{\theta_0} \quad (6)$$

and

$$P(Y_j|Y_0 = 0) = \frac{-\rho\sqrt{\theta_j(1-\theta_j)\theta_0(1-\theta_0)} + \theta_j(1-\theta_0)}{(1-\theta_0)}. \quad (7)$$

Note that, since $P \leq 1$, it follows from Eq. 7 that

$$\theta_j \geq \frac{\rho^2 \frac{\theta_0}{1-\theta_0}}{1 + \rho^2 \frac{\theta_0}{1-\theta_0}}, \quad (8)$$

and similarly for $0 \leq P$ and Eq. 6.

The results in Table 1 show that this non-identical, dependent model has the lowest bias, but the highest standard deviation. This sums of up much of Table 1, where more complex, and therefore more realistic, models reduces the bias but increases the variances.

Figure 5b shows the impact of correlation for non-identical classifiers. The bias decreases slowly for low correlations, but the rate increases as ρ_0 increases. Note that Eq. 8 restricts $d = b - a$, and the graphs are right-truncated. From Figure 4a we see that the impact from number of classifiers flattens off, and instead of restricting ρ_0 in our model, we can exclude classifiers by performance without large effect on the estimated bias. That is, restricting d instead of ρ_0 . What we also observe in Figure 5a is that change in d has less impact on the higher end of the scale, so this also supports a decision of excluding teams with low performance without impacting the bias estimation too much.

5 Real world examples

As we have shown above, the sample maximum is an overoptimistic estimate for SOTA. These results are based on known SOTA, but faced with real world data the problem is of

opposite nature: The sample maximum is known, but SOTA must be estimated. In the public challenge or public data set context there are many factors that come in to play, making bias calculations everything but straightforward.

We here demonstrate different aspects of real world analysis through SOTA estimation of three different cases: Obesity Risk (5.1.1), Cassava Leaf (5.1.2), and Melanoma (5.2.3). Obesity Risk and Cassava Leaf have accuracy, defined as $\hat{\theta}$, as their ranking criterion, whereas Melanoma has the more common AUC, the area under the receiver operating characteristic (ROC) curve, as ranking criterion. Estimating multiplicity effect on the AUC's is not as straightforward as with accuracy, but the mechanisms are the same.

5.1 Estimating θ_{SOTA}

In a public challenge with m participating teams, let $\hat{\Theta} = \{\hat{\theta}_1, \hat{\theta}_2, \dots, \hat{\theta}_m\}$ be the estimated probability of success for classifiers $j = 1, \dots, m$ based on the performance on an independent test sample of size n . The winning team is identified by the sample maximum, $\max(\hat{\Theta})$. Among the different scenarios presented in Section 4, the non-identical dependent is the most realistic model. Whereas in Table 1 we report $E\hat{\theta}_{\max}$ from known $P(\theta)$, the task is now to estimate θ_{SOTA} based on $\hat{\Theta}$.

A straightforward approach is to propose a distribution $\theta'_j \sim P(\theta')$ whose expected sample maximum equals the observed sample maximum, $E\max(\hat{\Theta}'(\mathbf{X})) = \max(\hat{\Theta})$. Deciding on $P(\theta')$ is a crucial part, and we use an empirical Bayes approach, where we estimate $P(\theta')$ from $\hat{\Theta}$. We base our suggested $P(\theta')$ on shrinking the sample estimates, as seen in Figures 8c and 11a, so that $E\max(\hat{\Theta}'(\mathbf{X})) = \max(\hat{\Theta})$. The shrink parameter is found numerically. Cropping, an alternative approach, gave similar results to shrinking, and the results are presented in the Appendix.

An alternative to the expected value is the upper limit of the 95% CI. The latter is more in line with common practices in research, and which to choose will depend on the aim of the analysis. We demonstrate the impact in the Obesity Risk example, reported in Table 2.

Not every $\max(\hat{\Theta})$ is a result of multiplicity, and we demonstrate this in the Cassava Leaf example.

5.1.1 MULTI-CLASS PREDICTION OF OBESITY RISK

Multi-Class Prediction of Obesity Risk is a challenge in the 2024 Kaggle Playground Series, using a synthetic data set generated from the *Obesity or CVD risk* data set (Palechor and de la Hoz Manotas, 2023). The test sample size was $n = 13,840$, and the number of teams were $m = 3,558$, excluding teams with accuracy lower than chance. Figure 8a shows the sample estimates, $\hat{\theta}_j$'s, zoomed in at the classifiers with sample estimates above 0.88 for better visualisation. The maximum sample estimate is $\hat{\theta}_{\max} = 0.9116$, shown as the vertical dotted magenta line in all subfigures of Figure 8 together with the $\hat{\theta}_j$'s in gray, for reference.

The 95% CI for the single $\hat{\theta}_{\max}$ is shown as the magenta horizontal line in Figure 8a, enveloping 921 teams. This should raise suspicion that the right tail seen in Figure 8a can be the product of multiplicity.

To demonstrate the impact of ignoring the multiplicity effect, we set the proposed distribution $\theta'_1, \dots, \theta'_m$ equal to the sample estimates, $\hat{\theta}_j$'s, and calculate the expected value of the sample maximum, $E\max(\hat{\Theta}')$. We use the set-up from Section 4.3 with correlation

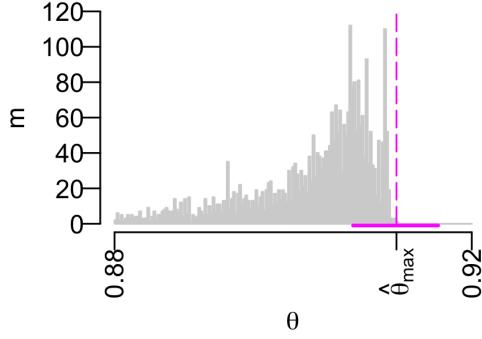
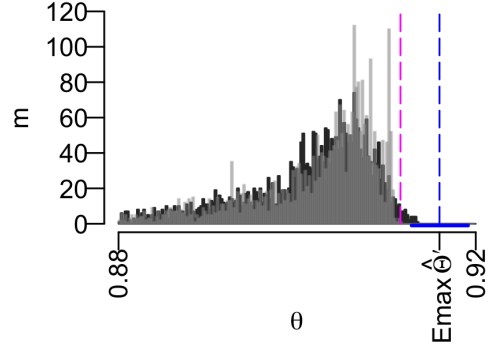
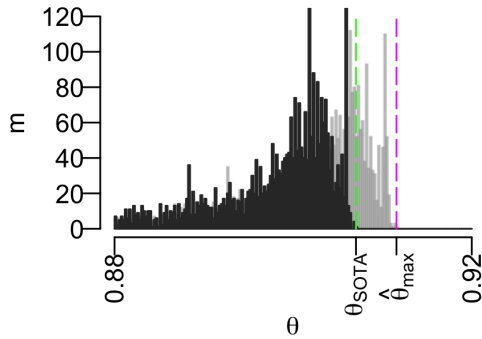
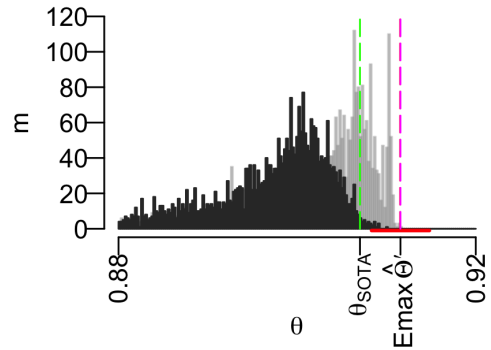
Obesity risk: Θ' and corresponding realisations(a) $\hat{\theta}_{\max}$ and its CI. Row 1, Table 2(b) A realisation from a), $E\max(\hat{\Theta}')$ and its CI. Row 2, Table 2.(c) Shrunk data, Θ' , and the new θ_{SOTA} (green). Row 3, Table 2.(d) A realisation from c), $E\max(\hat{\Theta}') = \hat{\theta}_{\max}$ and its CI (red). Row 3, Table 2.

Figure 8: The upper row shows the sample estimates and a corresponding realisation. The lower row shows a shrunk version and a corresponding realisation. For exact numbers, see Table 2. $\hat{\Theta}$ (gray) and $\hat{\theta}_{\max}$ (magenta) for reference.

coefficient $\rho_0 = 0.6$, and $P(Y_0) = \theta_0 = \max(\Theta')$. Note that sample estimates with low values are excluded in accordance with Eq. 8, but their influence on the expected maximum is negligible. A realisation is shown in Figure 8b. The upper tail, whose tip represents the maximum sample estimate, is stretched according to the variances of the Y_j s. The expected sample maximum is $E\max(\hat{\Theta}') = 0.9159$, far above the sample maximum in the challenge. The 95% CI is reported in Table 2. The lower bound exceeds $\max(\hat{\Theta})$, and we can conclude that the sample maximum is an unlikely candidate for SOTA.

Instead, we can find a set Θ' that results in realisations, $\hat{\Theta}'$, similar to the challenge sample estimates in terms of sample maximum, and let $\max(\Theta')$ be the SOTA candidate. To obtain a set Θ' where $E\max(\hat{\Theta}') = \max(\hat{\Theta})$, we shrink the challenge sample estimates

$$\theta'_j = w \cdot \hat{\theta}_j + (1 - w) \cdot \frac{1}{|\text{classes}|}, \quad (9)$$

where $|classes|$ is the number of classes, and $0 \leq w \leq 1$. The shrinking point, $1/|classes|$, is the random classifier. The weight, w , balances between the observations and the random element. Figure 8c shows the proposed Θ' . Figure 8d shows one realisation of the shrunk distribution, where $\max(\hat{\Theta}')$ coincides with $\max(\hat{\Theta})$, and the corresponding CI. The empirical Bayes distribution, with $E \max(\hat{\Theta}') = \max(\hat{\Theta})$, has $\max(\Theta') = 0.9070$ and this serves as a new candidate for the SOTA.

It can be argued that the new SOTA candidate is at risk of being an optimistic estimate, since the challenge observations are from only one test sample. The upper bound of the 95% CI can mitigate such a risk, and the challenge sample estimates are shrunk to fit that criterion. The results are shown in row 4 in Table 2.

Estimating θ_{SOTA}

Approach	$\max(\Theta')$	95% CI	$E \max(\hat{\Theta}')$	# teams
no mult.	$\hat{\theta}_{\max}$	(0.9067, 0.9162)	-	-
$\Theta' = \hat{\Theta}$	$\hat{\theta}_{\max}$	(0.9128, 0.9191)	0.9159	-
shrinking	0.9070	(0.9084, 0.9148)	$\hat{\theta}_{\max}$	841
	0.9036	(0.9050, $\hat{\theta}_{\max}$)	0.9082	1726

Table 2: The 95% CI and the expected value for sample maximum, $\max(\hat{\Theta}')$, for different SOTA estimation strategies, where SOTA is defined as $\max(\Theta')$. The challenge sample maximum is $\hat{\theta}_{\max} = 0.9116$. The rightmost column shows number of classifiers with sample performance above the estimated SOTA.

Table 2 demonstrates that taking the effect of multiplicity into account changes how results are perceived. The new SOTA value is 0.9070, and even though its reduction from best performance is less than 0.005, the effect it has on who we consider performing at SOTA-level is dramatic: around a quarter of the classifiers have sample performance above the new SOTA. The more conservative approach using the upper bound of the 95% CI to estimate SOTA gives an even more dramatic result, and either way the impact is substantial.

5.1.2 CASSAVA LEAF DISEASE

In this example, the maximum sample estimate is unlikely to be the product of multiplicity. For *The Cassava Leaf Disease Classification* challenge (Mwebaze et al., 2020), the task was to classify images of cassava leaves. The training sample consisted of 21,367 images of five classes, and the test sample of approximately 15,000 images. 3,752 teams participated, excluding those with sample performance lower than chance.

The three top performances appear as outliers: 0.9132, 0.9043 and 0.9028 as seen in Figure 9a. Several explanations for the outlying performances have been put forward, and the interested reader can take a deep-dive in the comment section of the challenge. Since this is not the topic of the present work, we will not engage in the discussion here. The 95% CI of $\hat{\theta}_{\max}$ is (0.9086, 0.9177), no other performance is within this interval. Already here we can decline a multiplicity-induced bias as a likely model.

We can take one more step, and set $\Theta' = \hat{\Theta}$. We get $E \max(\hat{\Theta}') < \hat{\theta}_{\max}$, and although the upper tail is stretched, its tip does not surpass $\hat{\theta}_{\max}$, as illustrated in Figure 9b.

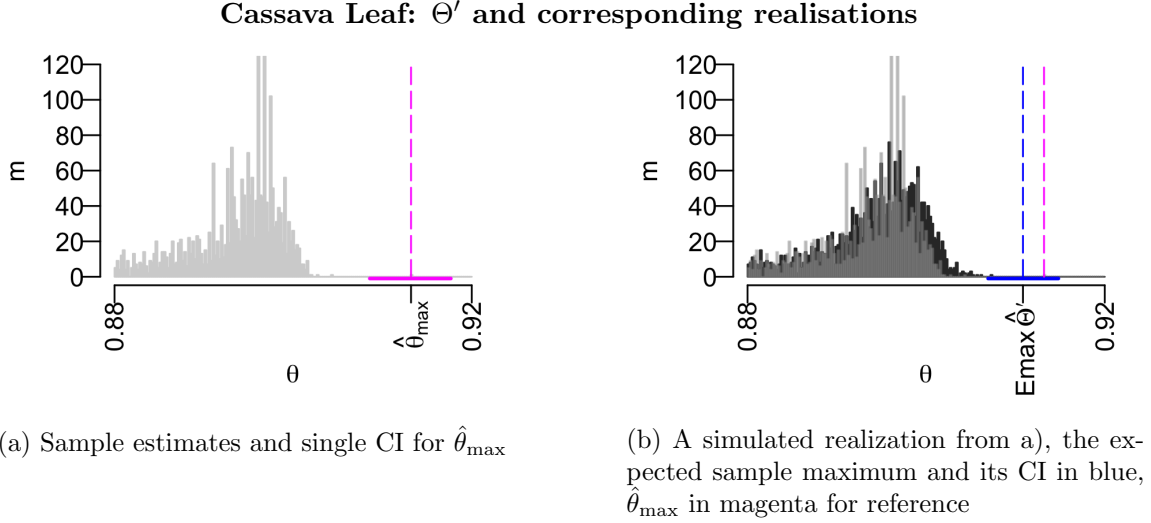


Figure 9: Cassava Leaf sample estimates as observed, and a corresponding simulated realisation.

It is easy to see that the proposed shrinkage model in Eq. 9 does not have a solution with the restriction that $E \max(\hat{\Theta}') = \hat{\theta}_{\max}$. This demonstrates how the suggested approach is inapplicable in an example where it is clearly not suited.

5.2 Estimating AUC_{SOTA}

In the following sections, we introduce a strategy for estimating AUC_{SOTA} , using simulated examples and the Melanoma Challenge for illustration.

5.2.1 SIMULATION OF AUC

In a binary classification problem, the calculation of AUC is based on scores of random variables from the positive and the negative class. The AUC is mathematically equivalent to the probability that a random variable from the positive class will be ranked higher, in terms of score, than a random variable from the negative class (Hanley and McNeil, 1982).

Let $score(\cdot)$ be a function that assigns a score to a random variable. Let $S_+ = score(W_+)$, where W_+ is a random variable from the positive class, and $S_- = score(W_-)$, where W_- is a random variable from the negative class. The distribution of classifier scores, S , is a mixture distribution of the S_+ and the S_- distributions, where the weights, π and $1 - \pi$, correspond to the probability of drawing a positive or a negative random variable, and has pdf

$$\pi f_+(s) + (1 - \pi) f_-(s),$$

where $f_+(s)$ and $f_-(s)$ are the pdfs of the positive and the negative class, respectively.

Then $AUC = P(S_- < S_+) = P(S_- - S_+ < 0)$, which is equivalent to the cdf at value 0. To simulate classifier scores according to a given $AUC = a$, we need to specify distributions for the variables S_-, S_+ in such a way that $P(S_- - S_+ < 0) = a$. We use

Normal distributions for illustration. Let S_+ and S_- have the distributions

$$\begin{aligned} S_+ &\sim \mathcal{N}(\mu_+, \sigma_+^2) \\ S_- &\sim \mathcal{N}(\mu_-, \sigma_-^2), \end{aligned}$$

where $\mathcal{N}(\mu, \sigma^2)$ is the Normal distribution with mean μ and variance σ^2 . We then have that

$$\text{AUC} = \Phi \left(\frac{0 - (\mu_- - \mu_+)}{\sqrt{\sigma_-^2 + \sigma_+^2}} \right), \quad (10)$$

where Φ is the cdf of the standard Normal distribution.

Figure 10a shows an example of two Normal distributions with means and variances chosen so that $\text{AUC} = 0.90$. The rugs show a sample of size $n = 3,000$ from the corresponding mixture distribution with $\pi = 0.017$. The observations can be visualised as an ROC curve, and Fig 10b shows curves for $m = 1,000$ samples. We consider the observed AUC for each sample, $\hat{\text{AUC}}_j$, $j = 1, \dots, m$, to be the sample estimates, analogous to $\hat{\Theta} = \{\hat{\theta}_1, \dots, \hat{\theta}_m\}$ in Section 3.3. The sample maximum AUC is $\max(\{\hat{\text{AUC}}_1, \hat{\text{AUC}}_2, \dots, \hat{\text{AUC}}_m\})$, and is displayed as the black line in Fig 10b. Figure 10c shows a simulated distribution of the sample maximum where the sample maximum from Fig 10b is close to its expected value.

5.2.2 SIMULATION RESULTS FOR UNCORRELATED CLASSIFIERS

To demonstrate the impact that multiplicity can have, we start with a simulated example similar to the one in Section 3.4. Consider a classification problem with $n = 3,000$, $m = 1,000$, where each classifier has an AUC of $a = 0.90$, and the classifiers are independent.

Whereas the distribution of the sample maximum for probability of success is independent of class balance as long as the probability of success is independent of class, this is not true for the sample maximum of AUC, where the variance increases with class imbalance. We have chosen the same class balance as in the Melanoma challenge, $\pi = 0.017$, as this reflects real world examples. For simplicity we choose $\mu_- = 0$ and $\sigma_- = \sigma_+ = 1$. As we see from Eq. 10 the AUC is completely decided by the ratio between the difference in means and the pooled standard deviation. Changing the scale of one implies the same change of scale in the other. Perhaps the strongest assumption is that of equal variances, but we see unrealistically variable AUCs from letting the difference between the two be too large, so keeping them equal was the simplest choice. We then solve for μ_+ numerically. Now we can generate scores from the resulting Normal distributions.

Figure 10c shows the simulated distribution of the sample maximum AUC over 10,000 repetitions of a challenge where every classifier has AUC of 0.90. The simulated expected value is 0.9562, the standard deviation is 0.004459, and the simulated 95% CI is (0.9486, 0.9662). Comparing this to the results in the upper row of Table 3, we see that the bias is much larger for the sample maximum AUC. This is partly due to the large variance created by the class imbalance. Although the sample size is $n = 3,000$, only 51 of those belong to the positive class, creating large variance in the estimator.

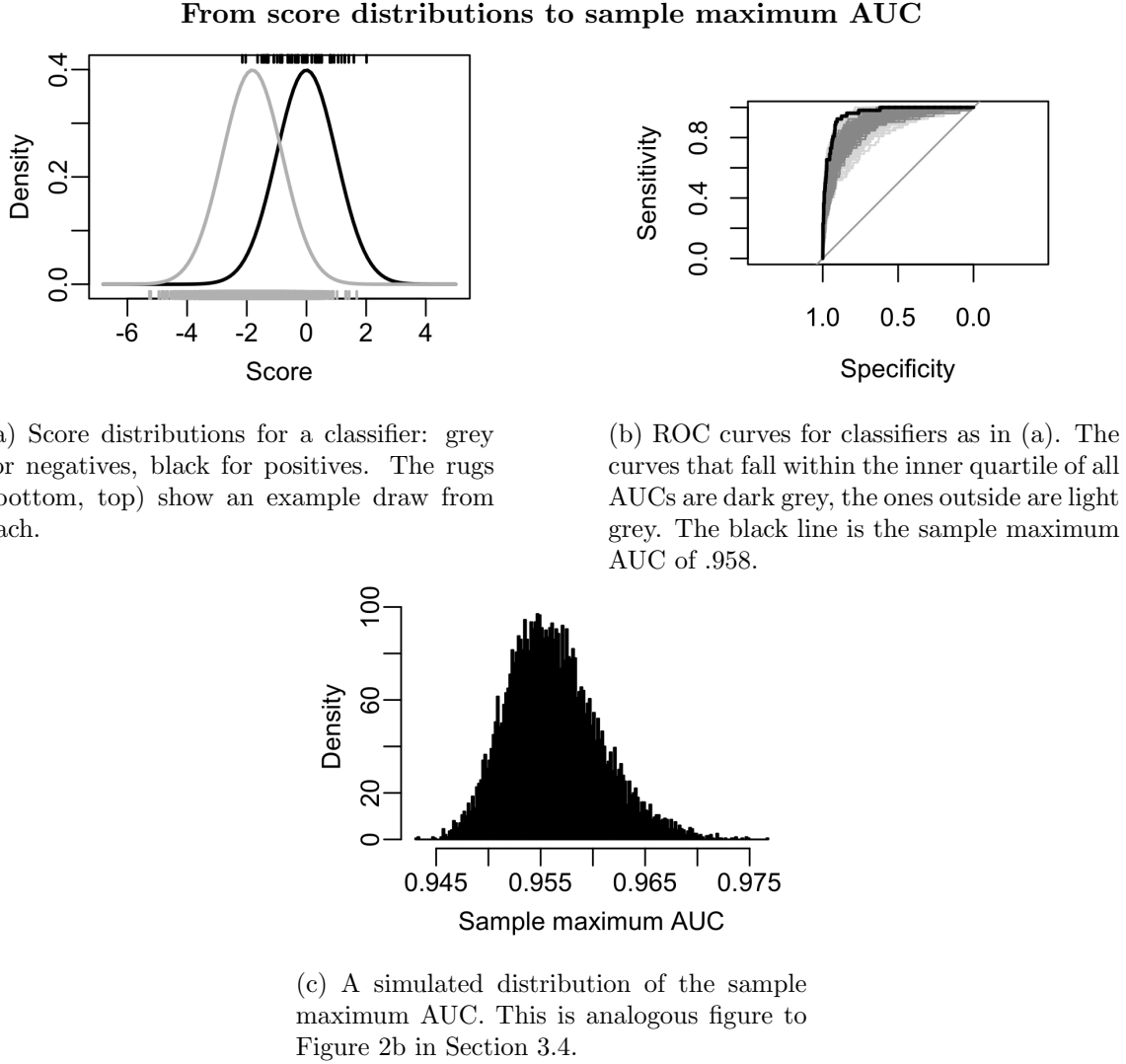


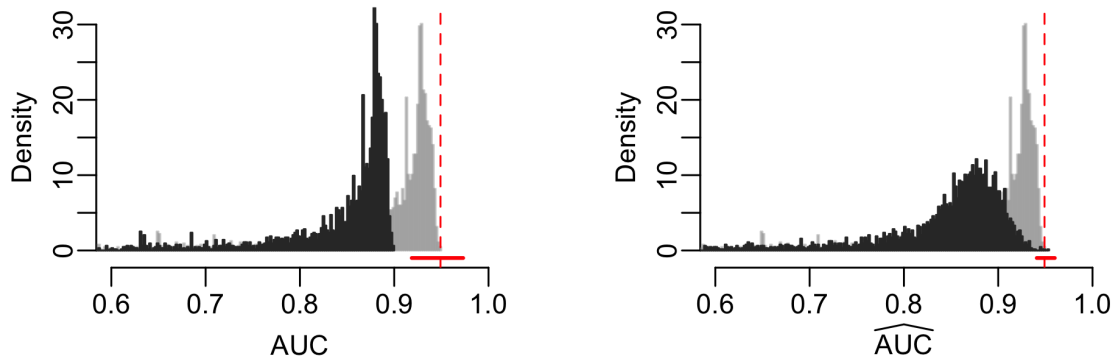
Figure 10: Example of what $AUC = 0.90$ might look like in practice for $\pi = 0.017$, $n = 3\,000$ and $m = 1\,000$. (a) shows the pdfs, (b) shows ROC curves of $m = 1\,000$ samples of (a), and (c) shows 10 000 simulations of sample maximums of (b).

5.2.3 MELANOMA CLASSIFICATION

We will use the Melanoma Classification challenge from 2020 as an illustrative example of AUC_{SOTA} estimation because it follows many of the common structures of public challenges.

The SIIM-ISIC Melanoma Classification (Zawacki et al., 2020) challenge consisted of more than 40,000 images of skin lesions from various sites, split into training (33,126), validation (3,295) and test set (7,687). The data set is highly imbalanced, with less than 2% melanomas, which reflects the reality in many cancer detection situations. A full description can be found in Rotemberg et al. (2021). The size of the test set is smaller than the recommendations of, for example, Roelofs et al. (2019), but reflects the reality of benchmark

Use of shrinkage distribution to suggest a SOTA



(a) Shrinkage AUC distribution (black) based on the Melanoma challenge results (grey). The vertical red line shows the highest Melanoma challenge AUC of .949 and the horizontal red line shows a 95% CI around this.

(b) A sample from the shrinkage distribution of (a). The vertical line is the expected sample maximum, engineered to coincide with the observed Melanoma challenge maximum of 0.949. The horizontal line shows the 95% CI of the sample maximum.

Figure 11: Histograms for AUC sample estimates shrunk toward 0.5. In the shrinkage distribution the state of the art is an AUC of 0.8992 which leads to the expected sample maximum AUC of 0.9490. AUCs below .6 not shown to make the more interesting upper region more readable.

datasets and public challenges, as seen in, for example, the overview of Willemink et al. (2020). We want to emphasise that the shortcomings of this challenge are not unique, and that is precisely why it serves as a useful example.

The prize money was set to 10,000 USD for the best-performing method, measured as AUC on the test set. Figure 11a shows the results. The team ‘All Data Are Ext’, consisting of three Kaggle Grandmasters, won the challenge, achieving an AUC of 0.9490, and their method and strategy is explained in Ha et al. (2020). Although we show that the AUC is an optimistic estimate for the melanoma detection SOTA, we do not question their rank in the challenge. Quite the contrary; the winning team chose many of the verified strategies from Section 2. They used additional data from previous years’ challenges, and they also did data augmentation. They chose ensemble learning as a strategy to avoid overfitting, a strategy implicitly supported by Talagrand (1996). They also trained on multiple classes, a strategy that Feldman et al. (2019) showed will slow down the overfitting.

The observed maximum is an unlikely SOTA candidate, and to give a better estimate of the SOTA for the Melanoma challenge, we follow the same procedure as in Section 5.1: The challenge observations are shrunk in such a manner that simulating from the shrunk set, AUC' , gives an expected sample maximum AUC of 0.9490, the challenge sample maximum.

Figure 11a shows the AUCs of the Melanoma challenge test sample shrunk toward 0.5, with maximum 0.8992. Figure 11b shows a corresponding sample, where the maximum is close to 0.9490. There are 2013 teams with performance above the new SOTA candidate. The discrepancy between the sample maximum and the new SOTA candidate is big and

has big implications. From an AUC close to 95% to barely 90% is a substantial drop in performance. Almost two thirds of the classifiers have performances above the new SOTA estimate.

As was shown in Section 4, illustrated in Figure 5b, the bias is reduced for correlated classifiers, so the analysis assuming independence overestimates the bias. In this challenge, we can assume multiple sources of dependency: Access to the same training set, models pre-trained on the same data, similar models, etc. However, the wide CI for a single classifier tells the story of an estimator with large variance, and hence the bias of the sample maximum will nevertheless be substantial.

5.3 Future work

There are several interesting aspects that has not been addressed in this work, that the authors briefly touched upon while preparing the manuscript.

5.3.1 CORRELATION BETWEEN CLASSIFIERS IN THE AUC SIMULATIONS

For the moment, we have not extended our AUC simulations to include correlations, but it should be possible to adopt a similar setup as in Sections 4.2 and 4.3: each classifier produces scores that correlate to those of a reference classifier. Let S_{0+} and S_{0-} be the scores of the reference classifier, for random variables from the positive and negative class, respectively.

Let $\rho_+ = \text{corr}(S_{0+}, S_{j+})$ be the correlation between the reference classifier scores S_{0+} and the scores of classifier j , S_{j+} for the positive class. If they both follow Normal distributions as outlined above, then the bivariate distribution is

$$\begin{pmatrix} S_{0+} \\ S_{j+} \end{pmatrix} \sim \mathcal{N} \left(\begin{pmatrix} \mu_{0+} \\ \mu_{j+} \end{pmatrix}, \begin{pmatrix} \sigma_{0+}^2 & \rho\sigma_{0+}\sigma_{j+} \\ \rho\sigma_{0+}\sigma_{j+} & \sigma_{j+}^2 \end{pmatrix} \right),$$

and equivalently for the negative class. However, the joint distribution of (S_0, S_j) is not uniquely defined by the correlation, and additional assumptions must therefore be made.

I

5.3.2 APPROXIMATE BAYESIAN POSTERIOR FOR SOTA

In Section 5 we consider observed data, \mathbf{x} , as coming from a hierarchical model like that of Figure 1 and try to find a $P(\theta)$ with expected maximum coinciding with $\max(\mathbf{x})$.

If we frame this as a Bayesian argument we could say that we are trying to find a prior that aligns well with our observed data and our model for the data. To find a prior we consider a very simple family of discrete distributions based on the empirical distribution of our data. In the usual Bayesian arguments the data model is expressed as a likelihood, $f(\mathbf{x} | \theta)$. We rely instead on simulations for the more complex models above.

We could instead consider a Bayesian analysis where we specify a prior for θ and try to find a posterior distribution for $\max(\theta)$. Approximate Bayesian Computation (Rubin, 1984) is quite close to what we do above in that instead of a likelihood the analysis uses a simulation of the data generating process.

Specifically we could specify some weakly informative prior, $P(\theta)$, simulate data, \mathbf{x}' , based on a draw, $\bar{\theta} \sim P(\theta)$, and check if $|\max(\mathbf{x}') - \max(\mathbf{x})| < \epsilon$ for some acceptable $\epsilon > 0$.

If yes, we consider $\max(\bar{\theta})$ a draw from the posterior distribution, $P(\max(\theta) \mid \mathbf{x})$, otherwise we discard it. Repeating this would give us a posterior distribution for $\max(\theta)$ without us having to specify some ad-hoc family of priors, requiring instead a single prior distribution and the specification of ϵ .

6 Discussion

Some of the insights presented here are obvious to anyone with a basic understanding of probability, like the introductory coin-flip example in Section 3.2. The mechanisms we have described are similar to those we find in regression to the mean, a well-known phenomenon in various fields such as livestock breeding and sport results. We believe that this has been neglected mainly because of the lack of formalisation: What is meant by SOTA performance, and what question does it answer? The main contribution has been to phrase the question, both the one that is commonly answered by reporting the maximum performance, and the question that can give an unbiased estimate of the SOTA performance.

Although our models span from the special case of iid classifiers to heterogeneous and correlated ones, the analysis is limited by the assumptions one has to make regarding distributions and correlation coefficients. An important lesson for practical applications is that simpler models tend to overestimate the bias, and hence underestimate the SOTA.

Looking at the application to real data in Section 5, we see that the implications of shifting the focus from best sample performance to best classifier performance has huge implications. Not necessarily so much in the new SOTA performance estimate, like the 0.005 shift in Section 5.1.1, but definitely in which classifiers we consider performing at SOTA level - in this example, 25% of the participating teams. In the Melanoma example in Section 5.2.3, the decrease in estimated SOTA performance is more striking, and we must keep in mind the wisdom from before, that simpler models tend to overestimate the bias. However, any model will uncover bias, and any bias will have quite dramatic results in terms of number of teams performing at SOTA level.

What does this mean for how we view the results from public challenges, such as Kaggle? First, we would like to emphasize that we appreciate the positive contributions that public challenges make, and that this is meant as a modification of how their results are viewed in the aftermath.

The beauty of the approach presented in this work - that we do not even have to know *which* classifier is the best to estimate the best performance - becomes the curse for the public challenge: We do not know which team is the best, only which was good combined with luck. The approach described here offers a method to quantify that luck, or *uncertainty* as we would name it in statistics. Like anyone with a basic understanding of probability can draw the conclusions in the coin-flip example, anyone with a basic understanding of statistics will look at the distribution of observed performances, as in Figure 8a, and suspect that the right tail is a product of sample variance. This work offers a way of connecting the dots from coin-flip to public challenge, and reveals some of the plentiful hurdles along that route.

In some fields of science, where hundreds of thousands of tests are performed simultaneously, the effects of multiplicity simply cannot be ignored. But as we see from Figures 4a

and 4b, this is not a thousand-classifier problem, it is a two-classifier problem. As soon as you have two classifiers, the observed maximum is appreciably biased.

It is obvious from Figure 8d that the chosen approach to find a good empirical distribution is not optimal. A sample from the empirical distribution in Figure 8c should ideally result in a sample similar to the observed sample estimates, that is, an overlap between the black and the gray histograms in Figure 8d. Whereas this is not that difficult to achieve, it requires more parameters and more tweaking, and does not result in any generalizable model. When deep-diving into a specific problem, it can be worthwhile spending some extra time refining those models, and presenting different results depending on model choice.

There are several approaches that can contribute to the problem of multiplicity, as presented in Section 2. Common for the solutions presented there are that they require additional data or more elaborate set-ups for public challenges. The approach presented here offers a tool that can be applied to already published results, and does not require convincing anyone else to change their preferred approach to finding the best solution.

Appendix A. Numerical results

Expected values and standard deviations for $\hat{\theta}_{\max}(\mathbf{X})$

m	n	θ	$E\hat{\theta}_{\max}$	$\sigma_{\hat{\theta}_{\max}}$
1,000	3,000	0.90	0.9173	0.001817
100	3,000	0.90	0.9135	0.002250
5,000	3,000	0.90	0.9196	0.001623
1,000	1,000	0.90	0.9294	0.003007
1,000	10,000	0.90	0.9096	0.001022
1,000	3,000	0.85	0.8707	0.002197
1,000	3,000	0.95	0.9624	0.001277

Table 3: The expected value and standard deviation for the SOTA estimator with varying test set size, number of classifiers and probability of success. Row 1 is the example used in Fig. 2. The subsequent rows correspond to the intersection between the gray vertical lines and the curves in Fig. 4.

Estimating θ_{SOTA} by cropping

Approach	$\max(\Theta')$	95% CI	$E \max(\hat{\Theta}')$	# teams
cropping	0.9063	(0.9084, 0.9148)	$\hat{\theta}_{\max}$	1134
	0.9026	(0.9050, $\hat{\theta}_{\max}$)	0.9083	1844

Table 4: The 95% CI and the expected value for sample maximum for SOTA estimation by cropping. This corresponds to the shrinking in Table 2. The standard deviations are in the order of magnitude 10^{-5} - 10^{-4} , and are therefore not displayed. The rightmost column shows number of classifiers with sample performance above the estimated SOTA.

References

- Aishwarya Agrawal, Dhruv Batra, Devi Parikh, and Aniruddha Kembhavi. Don’t just assume; look and answer: Overcoming priors for visual question answering. In *Proceedings of the IEEE conference on computer vision and pattern recognition*, pages 4971–4980, 2018.
- Craig M Bennett, Abigail A Baird, Michael B Miller, and George L Wolford. Neural correlates of interspecies perspective taking in the post-mortem atlantic salmon: An argument for multiple comparisons correction. *Neuroimage*, 47:S125, 2009.
- Avrim Blum and Moritz Hardt. The ladder: A reliable leaderboard for machine learning competitions. In *International Conference on Machine Learning*, pages 1006–1014. PMLR, 6 2015.
- Philip J. Boland, Frank Proschan, and Y. L. Tong. Modelling dependence in simple and indirect majority systems. *Journal of Applied Probability*, 26:81–88, 3 1989. ISSN 0021-9002. doi: 10.2307/3214318.
- Olivier Bousquet and André Elisseeff. Stability and generalization. *Journal of Machine Learning Research*, 2:499–526, 2002.
- Xavier Bouthillier, Pierre Delaunay, Mirko Bronzi, Assya Trofimov, Brennan Nichyporuk, Justin Szeto, Nazanin Mohammadi Sepahvand, Edward Raff, Kanika Madan, Vikram Voleti, Samira Ebrahimi Kahou, Vincent Michalski, Tal Arbel, Chris Pal, Gael Varoquaux, and Pascal Vincent. Accounting for variance in machine learning benchmarks. *Proceedings of Machine Learning and Systems*, 3:747–769, 3 2021.
- George Casella and Roger L. Berger. *Statistical Inference*. Duxbury, 2nd edition, 2002. ISBN 0-534-24312-6.
- Janez Demšar. Statistical comparisons of classifiers over multiple data sets. *Journal of Machine Learning Research*, 7:1–30, 2006.
- Thomas G. Dietterich. Approximate statistical tests for comparing supervised classification learning algorithms. *Neural Computation*, 10:1895–1923, 10 1998. ISSN 0899-7667. doi: 10.1162/089976698300017197.
- Cynthia Dwork, Vitaly Feldman, Moritz Hardt, Toniann Pitassi, Omer Reingold, and Aaron Roth. Guilt-free data reuse. *Communications of the ACM*, 60:86–93, 4 2017. ISSN 15577317. doi: 10.1145/3051088.
- Mark Everingham, S. M. Ali Eslami, Luc Van Gool, Christopher K.I. Williams, John Winn, and Andrew Zisserman. The pascal visual object classes challenge: A retrospective. *International Journal of Computer Vision*, 111:98–136, 1 2015. ISSN 15731405. doi: 10.1007/S11263-014-0733-5/FIGURES/27.
- Vitaly Feldman, Roy Frostig, and Moritz Hardt. The advantages of multiple classes for reducing overfitting from test set reuse. In *International Conference on Machine Learning*, pages 1892–1900. PMLR, 5 2019.

- Manuel Fernández-Delgado, Eva Cernadas, Senén Barro, Dinani Amorim, and Amorim Fernández-Delgado. Do we need hundreds of classifiers to solve real world classification problems? *Journal of Machine Learning Research*, 15:3133–3181, 2014.
- Odd Erik Gundersen and Sigbjørn Kjensmo. State of the art: Reproducibility in artificial intelligence. *Proceedings of the AAAI Conference on Artificial Intelligence*, 32:1644–1651, 4 2018. ISSN 2374-3468. doi: 10.1609/AAAI.V32I1.11503.
- David Gutman, Noel C. F. Codella, Emre Celebi, Brian Helba, Michael Marchetti, Nabin Mishra, and Allan Halpern. Skin lesion analysis toward melanoma detection: A challenge at the international symposium on biomedical imaging (isbi) 2016, hosted by the international skin imaging collaboration (isic), 2016. URL <https://arxiv.org/abs/1605.01397>.
- Qishen Ha, Bo Liu, and Fuxu Liu. Identifying melanoma images using efficientnet ensemble: Winning solution to the siim-isic melanoma classification challenge, 2020. URL <https://arxiv.org/abs/2010.05351>.
- J A Hanley and B J McNeil. The meaning and use of the area under a receiver operating characteristic (roc) curve. *Radiology*, 143(1):29–36, Apr 1982. ISSN 0033-8419 (Print); 0033-8419 (Linking). doi: 10.1148/radiology.143.1.7063747.
- Masato Hisakado, Kenji Kitsukawa, and Shintaro Mori. Correlated binomial models and correlation structures. *Journal of Physics A: Mathematical and General*, 39(50):15365, 2006.
- Daniel W. Ladd. An algorithm for the binomial distribution with dependent trials. *Journal of the American Statistical Association*, 70:333–340, 1975. ISSN 1537274X. doi: 10.1080/01621459.1975.10479867.
- Rachel Longjohn, Markelle Kelly, Sameer Singh, and Padhraic Smyth. Benchmark data repositories for better benchmarking. In *Proceedings of the 38th International Conference on Neural Information Processing Systems*, page 2744, 2025. ISBN 9798331314385.
- Zhiyi Ma, Kawin, Ethayarajh, Tristan Thrush, Somya Jain, Ledell Wu, Robin Jia, Christopher Potts, Adina Williams, and Douwe Kiela. Dynaboard: An evaluation-as-a-service platform for holistic next-generation benchmarking. *Advances in Neural Information Processing Systems*, 34:10351–10367, 12 2021.
- Horia Mania, John Miller, Ludwig Schmidt, Moritz Hardt, and Benjamin Recht. Model similarity mitigates test set overuse. *Advances in Neural Information Processing Systems*, 32, 2019.
- Ernest Mwebaze, Jesse Mostipak, Joyce, Julia Elliott, and Sohier Dane. Cassava Leaf Disease Classification. <https://kaggle.com/competitions/cassava-leaf-disease-classification>, 2020. Kaggle.

- Kajsa Møllersen, Maciel Zortea, Thomas R. Schopf, Herbert Kirchesch, and Fred Godtliebsen. Comparison of computer systems and ranking criteria for automatic melanoma detection in dermoscopic images. *PLOS ONE*, 12(12):1–11, 12 2017. doi: 10.1371/journal.pone.0190112. URL <https://doi.org/10.1371/journal.pone.0190112>.
- Fabio Mendoza Palechor and Alexis de la Hoz Manotas. Obesity or CVD risk, 2023. URL <https://www.kaggle.com/dsv/7009925>.
- Benjamin Recht, Rebecca Roelofs, Ludwig Schmidt, and Vaishaal Shankar. Do imagenet classifiers generalize to imagenet? In *International conference on machine learning*. PMLR, 5 2019.
- Rebecca Roelofs, Vaishaal Shankar, Benjamin Recht, Sara Fridovich-Keil, Moritz Hardt, John Miller, and Ludwig Schmidt. A meta-analysis of overfitting in machine learning. *Advances in Neural Information Processing Systems*, 32, 2019.
- Veronica Rotemberg, Nicholas Kurtansky, Brigid Betz-Stablein, Liam Caffery, Emmanouil Chousakos, Noel Codella, Marc Combalia, Stephen Dusza, Pascale Guitera, David Gutman, Allan Halpern, Brian Helba, Harald Kittler, Kivanc Kose, Steve Langer, Konstantinos Lioprys, Josep Malvehy, Shenara Musthaq, Jabpani Nanda, Ofer Reiter, George Shih, Alexander Stratigos, Philipp Tschandl, Jochen Weber, and H. Peter Soyer. A patient-centric dataset of images and metadata for identifying melanomas using clinical context. *Scientific Data* 2021 8:1, 8:1–8, 1 2021. ISSN 2052-4463. doi: 10.1038/s41597-021-00815-z.
- Donald B. Rubin. Bayesianly Justifiable and Relevant Frequency Calculations for the Applied Statistician. *The Annals of Statistics*, 12(4):1151 – 1172, 1984. doi: 10.1214/aos/1176346785.
- Steven L. Salzberg. On comparing classifiers: Pitfalls to avoid and a recommended approach. *Data Mining and Knowledge Discovery*, 1:317–328, 1997. ISSN 13845810. doi: 10.1023/A:1009752403260/METRICS.
- Michel Talagrand. A new look at independence. *The Annals of Probability*, 24:1–34, 1996.
- Damien Teney, Ehsan Abbasnejad, Kushal Kafle, Robik Shrestha, Christopher Kanan, and Anton van den Hengel. On the value of out-of-distribution testing: An example of goodhart’s law. *Advances in Neural Information Processing Systems*, 33:407–417, 2020.
- William Hedley Thompson, Jessey Wright, Patrick G. Bissett, and Russell A. Poldrack. Dataset decay and the problem of sequential analyses on open datasets. *eLife*, 9:1–17, 5 2020. ISSN 2050084X. doi: 10.7554/ELIFE.53498.
- Antonio Torralba and Alexei A. Efros. Unbiased look at dataset bias. *Proceedings of the IEEE Computer Society Conference on Computer Vision and Pattern Recognition*, pages 1521–1528, 2011. ISSN 10636919. doi: 10.1109/CVPR.2011.5995347.
- John W Tukey. The philosophy of multiple comparisons. *Statistical Science*, 6:100–116, 1991.

- Gaël Varoquaux and Veronika Cheplygina. Machine learning for medical imaging: methodological failures and recommendations for the future. *npj Digital Medicine* 2022 5:1, 5: 1–8, 4 2022. ISSN 2398-6352. doi: 10.1038/s41746-022-00592-y.
- Y. H. Wang. On the number of successes in independent trials. *Statistica Sinica*, 3:295–312, 1993.
- Martin J. Willemink, Wojciech A. Koszek, Cailin Hardell, Jie Wu, Dominik Fleischmann, Hugh Harvey, Les R. Folio, Ronald M. Summers, Daniel L. Rubin, and Matthew P. Lungren. Preparing medical imaging data for machine learning. *Radiology*, 295:4–15, 2 2020. ISSN 15271315. doi: 10.1148/RADIOL.2020192224/ASSET/IMAGES/LARGE/RADIOL.2020192224.FIG5B.JPEG.
- Anna Zawacki, Brian Helba, George Shih, Jochen Weber, Julia Elliott, Marc Combalia, Nicholas Kurtansky, NoelCodella, Phil Culliton, and Veronica Rotemberg. SIIM-ISIC Melanoma Classification. <https://kaggle.com/competitions/siim-isic-melanoma-classification>, 2020. Kaggle.